2017

Electromechanical Instability in Silicone-and Acrylate-based Dielectric Elastomers

Liang Jiang
Qingdao University

Yanfen Shou
Qingdao University

Shaojuan Chen
Qingdao University

Jianwei Ma
Qingdao University

Tony Betts
Technological University Dublin, anthony.betts@tudublin.ie

Follow this and additional works at: https://arrow.tudublin.ie/aegart

Part of the Physics Commons
See next page for additional authors

Recommended Citation

Authors

Liang Jiang, Yanfen Shou, Shaojuan Chen, Jianwei Ma, Tony Betts, and Stephen Jerrams

Electromechanical instability in silicone and acrylate based dielectric elastomers

Liang Jiang [1a], Yanfen Zhou [a], Shaojuan Chen [a], Jianwei Ma [a], Anthony Betts [b],

Stephen Jerrams [c]

[a] School of Textile and Garment, Qingdao University, Qingdao, Shandong, China

[b] Applied Electrochemistry Group, Focas Research Institute, Dublin Institute of Technology,

Dublin D08 NF82, Ireland

[c] Centre for Elastomer Research, Focas Research Institute, Dublin Institute of Technology,

Dublin D08 NF82, Ireland

Abstract

Electromechanical instability (EMI) is regarded as a significant factor in preventing dielectric elastomers (DEs) achieving large voltage-induced deformations. In this work, the strain-stiffening effect was used to control EMI in DEs. Results showed that the stretch ratio required to provide a feasible strain-stiffening effect in silicone rubber (SR) was smaller than that for a commercial DE material VHB 4910. Experimental data were compared with currently used models for the simulation of EMI in DEs. It was found that EMI could be eliminated in the deformation of these elastomers if pre-stretch was employed. By applying a pre-stretch ratio of above 2.0, EMI was suppressed in both VHB 4910 and SR samples. The findings of this research are of great significance in maximizing the electromechanical performance of DE materials.

1. Introduction

Dielectric Elastomers (DEs), which can respond to electrical stimuli by changing their shape, belong to the family of smart materials. The effective compressive stress (σ_v) is created by applying a high voltage between the top and bottom surfaces of a DE sample and complies with Eqn. (1) [1]. DEs have attracted increased attention because they offer the advantages of large voltage-induced deformation (> 380%), high energy density ($\approx$ 3.4 MJ/m^3) and high electromechanical coupling efficiency (> 85%) [2],

---

[1] Corresponding author, email: jiang.liang@outlook.com

combined with light weight, low cost and freedom from noise pollution [3-6]. Moreover, they are sometimes referred to as "artificial muscle" materials because they can readily resemble natural muscle under strain, as well as displaying similar actuation pressures, response speeds, electromechanical energy densities and coupling efficiencies. Consequently, DEs have been proposed for multiple applications in the fields of biomimicry [7, 8], artificial intelligence [9-11] and renewable energy [12, 13].

$$\sigma_V = \varepsilon' \varepsilon_0 \left(\Phi / h \right)^2 = \varepsilon' \varepsilon_0 \varphi^2 \qquad (1)$$

Where ε' is the relative permittivity of the DE material, ε_0 is the permittivity of the free space (8.85×10^{-12} F/m), φ is the electric field which equals the applied high voltage (Φ) divided by the thickness of the DE (h).

Generally, DEs can exhibit a high range of strains (10%–300%), but they require large electric fields (usually around 100 V/μm) to achieve high actuated strains [14]. Furthermore, electromechanical instability (EMI), which is also termed pull-in instability, is highlighted as the most significant failure mode for DEs when they are used as electromechanical actuators [15, 16]. This kind of failure occurs when the thickness of a DE falls below a certain threshold and the equivalent Maxwell pressure exceeds the compressive stress of the elastomer film. Its positive feedback leads to an unstable compression of the elastomer material which reduces the thickness further and consequently breakdown ensues [17]. Significantly, EMI has been observed to occur when an electric field is applied to the widely used commercial polyacrylate DE material, VHB 4910, which is manufactured and supplied by 3M (see Fig. 1). This has limited the material's ability to achieve large voltage-induced deformations [17, 18]. In addition, this polyacrylate film has the intrinsic drawbacks of low thermal stability, sensitivity to environmental degradation [19] and high viscoelasticity resulting in a relatively slow response to an electrical signal, thus limiting coupling efficiency [20, 21].
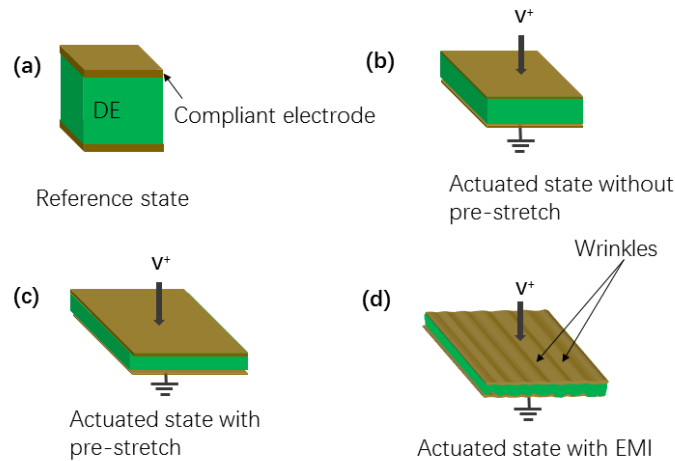
Fig. 1 An illustration of the DE working principle and the occurrence of EMI

It was reported that the operating electric field of a DE could be decreased by increasing a DE's dielectric constant and also through lowering the material's Young's modulus [22]. A soft silicone rubber (SR) not only has a low Young's modulus, but also has the advantages of low viscoelasticity, good thermal stability and improved biocompatibility when compared with most carbon-based polymers including the commercially available 3M VHB 4910 polyacrylate [19]. Though the dielectric constant of SR is relatively low ($\approx$ 2.9), it can be increased by incorporating nano/micron sized high-dielectric filler particles into the DE matrix [23, 24].

It has also been shown that pre-stretch offers numerous advantages in improving the properties of DEs when the material is subjected to large voltage-induced deformations, such as decreasing the viscoelastic (time-dependent) behaviour of VHB 4910, improving the material's actuation performance, dielectric strength, response speed and eliminating EMI. Zhao et al. [25] studied the mechanism of EMI and found that it could be delayed by tuning the stiffness of DEs using mechanical pre-stretch. The Suo model has been widely used to investigate EMI in DEs [26] and Li [27] developed a new model by considering the influence of stretch on the dielectric constant of DE materials. In this work, the EMI of two kinds of DEs, SR and VHB 4910, has been studied when samples of each were subjected to equi-biaxial stretch. Experimental data were compared with modeling results to provide an insight into the electromechanical performance of SR and VHB 4910 when undergoing EMI.

2. Materials and methods

2.1 Sample preparation

Two kinds of hyperelastic DE materials were chosen for this research. A commercial silicone polymer, dimethylsiloxane (LSR 4305 DEV, Bluestar Ltd., U.S.A), consisting of two parts (part A and part B) was used to fabricate silicone rubber based DE samples; a commercial DE, VHB 4910; a polyacrylate from the 3M company UK, having a thickness of 1 mm, was also employed. NYOGEL 756G (Nye Lubricants, Inc., USA), a conductive carbon grease, was used as the compliant electrode for both SR based DEs and VHB4910.

2.2 Mechanical tests

The bubble inflation test system was used to induce dynamic equi-biaxial mechanical stresses in DE samples by hydraulically inflating and deflating them using inert silicone oil as inflation medium. Disc samples of 2 mm thickness and 50 mm nominal diameter were prepared for equi-biaxial testing. The samples were held in the bubble inflation system's inflation orifice, as shown in Fig .2. In static tests, pressure was applied to the samples causing them to inflate. During inflation (or deflation) the system's vision system used two complementary metal-oxide semiconductor (CMOS) cameras to record the movement of the centres of specific points aligned at the pole on the surface of each sample. Stress values were simultaneously derived from the applied pressure and bubble geometry, with strain (or stretch ratio) values calculated from the change in circumferential distance between the centres of the points on the bubble surface using three-dimensional position coordinates obtained from the vision system output. Hence, the relation between stress and strain (or stretch ratio) was obtained in real time.
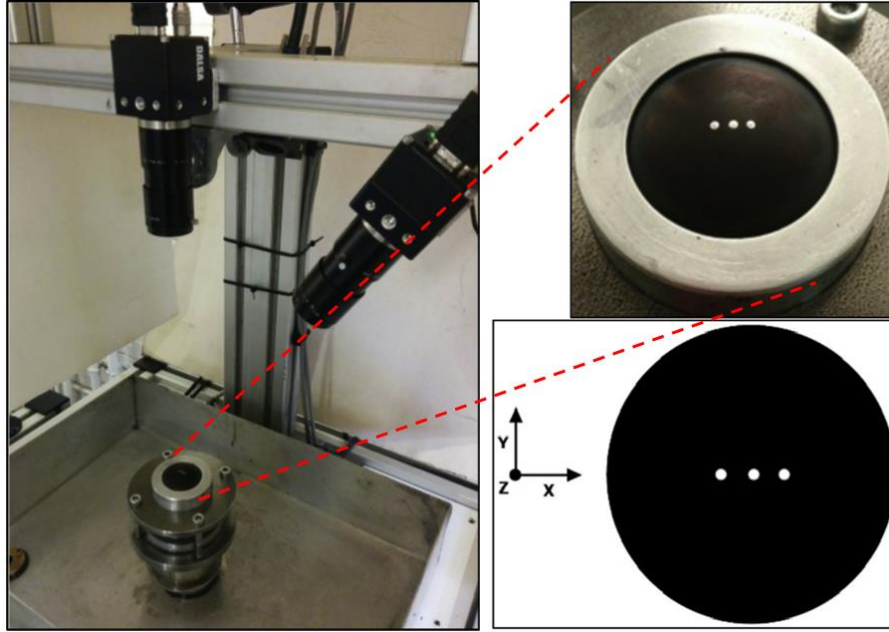
Fig. 2 Inflation orifice for bubble inflation test

2.3 Dielectric tests

Broadband dielectric spectroscopy was carried out on samples at 20°C in the frequency range from 100 Hz to 10 MHz using a Turnkey broadband dielectric spectrometer. The cell was a disposable gold-plated flat electrode with a diameter of 20 mm and a thickness of 2 mm. Samples were placed in the gap between the electrode and the sample holder.

2.4 Electromechanical tests

The electromechanical test system consists of a camera, a biaxial pre-stretching clamp and a high voltage power supply. Samples of 0.3 mm thickness were coated with the compliant electrode. The samples were clamped with a pre-stretch ratio of 1.6 applied to them. The camera recorded changes in the area of the compliant electrode when an electric field was incrementally applied in voltage steps of 0.5 kV. Thereafter, the initial area (A_0) and the actuated area (A) were accurately measured using AutoCAD software. The area strain s_a was calculated from the following expression.

$$s_a = (A - A_0)/A_0 \qquad\qquad (2)$$

3. The theory of EMI for hyperelastic DEs

Incompressible or nearly incompressible isotropic materials, such as rubber and muscle

fiber, are capable of undergoing large reversible elastic deformations and are often characterised by a strain energy function per unit volume denoted by W [28, 29]. One type of function is obtained from symmetry, thermodynamics and energy considerations and depends upon the three simplest even powered strain invariants (I_1, I_2, I_3) for the material [30]. Hence:

$$W = W(I_1, I_2, I_3) \qquad (3)$$

The strain energy function of Eqn. (3) can be replaced by means of a Lagrange multiplier [31] to give:

$$W(I_1, I_2, I_3) = W(I_1, I_2) - \frac{P}{2}(I_3 - 1) \qquad (4)$$

where

$$I_1 = \lambda_1^2 + \lambda_2^2 + \lambda_3^2 \qquad (5)$$

$$I_2 = \lambda_1^2 \lambda_2^2 + \lambda_2^2 \lambda_3^2 + \lambda_1^2 \lambda_3^2 \qquad (6)$$

$$I_3 = \lambda_1^2 \lambda_2^2 \lambda_3^2 = 1 \qquad (7)$$

As the strain invariants depend on principal stretches (λ_1, λ_2, λ_3), the expression for strain-energy may alternatively appear as a function of stretches:

$$W(I_1, I_2) = W(\lambda_1, \lambda_2, \lambda_3) \qquad (8)$$

Generally, for an incompressible material under uniaxial elongation, $\lambda_1 = \lambda$ and $\lambda_2 = \lambda_3 = \lambda^{-0.5}$. This allows the three simplest even powered strain invariants to be expressed as:

$$I_1 = \lambda^2 + \frac{2}{\lambda} \qquad (9)$$

$$I_2 = 2\lambda + \frac{1}{\lambda^2} \qquad (10)$$

$$I_3 = 1 \qquad (11)$$

whereas for equi-biaxial tension, the principal stretches are $\lambda_1 = \lambda_2 = \lambda$ and $\lambda_3 = \lambda^{-2}$, hence:

$$I_1 = 2\lambda^2 + \frac{1}{\lambda^4} \qquad (12)$$

$$I_2 = \lambda^4 + \frac{2}{\lambda^2} \qquad (13)$$

$$I_3 = 1 \qquad (14)$$

Meanwhile, the true stress-strain relationship $\sigma(\lambda)$ for elastomers can be derived from a strain-energy density function ($W(\lambda)$) [32] as shown in Eqn. (15).

$$\sigma(\lambda) = \lambda \frac{\partial W(\lambda)}{\partial \lambda} \qquad (15)$$

According to Suo's theory [33], the applied voltage Φ is a function of stretch λ which can be obtained from Eqn. (16) [34].

$$\sigma_{pre} + \sigma_V = \sigma(\lambda) \qquad (16)$$

where the membrane is subjected to a fixed force P and is mechanically pre-stretched to a ratio λ_{pre} corresponding to a stress $\sigma_{pre} = P/h\lambda_{pre}$; $\sigma(\lambda)$ is the true stress related to stretch. Combined with Eqn. (17), $\Phi(\lambda)$ can be determined using the expression:

$$\Phi(\lambda) = H\lambda^{-2}\sqrt{(\sigma(\lambda) - \sigma_{pre})/\varepsilon'\varepsilon_0} \qquad (17)$$

In previous research, it was considered that this minimal influence could be ignored [41]. Recently, it was found that pre-stretch had a significant influence on the dielectric constant of VHB 4910 [27, 35]. However, the dielectric constant of SR was virtually unchanged during pre-stretch in the experiments described here. In Li's work [27], the relation between equi-biaxial stretch and dielectric constant of VHB 4910 $\varepsilon(\lambda)$ was summerised using the following equation (Eqn. (18)). The electrostrictive coefficients a, b and c in the equation were determined by fitting the experimental data. Typical values were $a = -0.2908$, $b = 0.0902$, $c = -0.0098$.

$$\varepsilon(\lambda) = \varepsilon_0\varepsilon'\left(1 + 2a(\lambda - 1) + 4b(\lambda - 1)^2 + 8c(\lambda - 1)^3\right) \qquad (18)$$

If this expression is substituted in Eqn. (17), Eqn. (19) can be determined.

$$\Phi(\lambda) = H\lambda^{-2}\sqrt{(\sigma(\lambda) - \sigma_{pre})/\left(\varepsilon_0\varepsilon'\left(1 + 2a(\lambda - 1) + 4b(\lambda - 1)^2 + 8c(\lambda - 1)^3\right)\right)} \qquad (19)$$

A theoretical analysis has been incorporated into the research described in this paper to describe the relation between applied voltage and actuated stretch ratio. Consequently, an explanation for the occurrence of EMI in DEs is given.

4. Results and discussion

In DEs the value of the measured dielectric constant is dependent upon a number of factors; principally the chemical composition and electronic structure of the elastomeric material. Bond energies and bond lengths as well as bond angles can all have an

influence, as can differences in electronegativities between adjacent bound atoms comprising the molecular chains. In this case, the two dielectric elastomers utilise carbon-based (VHB 4910) and silicon-based (SR LSR 4305) polymeric units, which display very different characteristics in an imposed electric field. The dielectric spectra of VHB 4910 and the silicone composites at 20°C are shown in Fig 3. As can be seen from the figure, the dielectric constant of VHB 4910 was about 4.7 at 1 kHz. Over the test range, it decreased gradually from 4.8 to 3.5 with increases in frequency. However, the dielectric constant for pure SR, which is about 2.9, appeared to be independent of frequency. By comparison with VHB 4910, the permittivity of SR LSR 4305 is lower, because the polyacrylate contains a strong carbonyl group (-C=O) which has a much higher bond energy and is much more polar than any other Si-O, Si-C, Si-H (silicon) or C-O, C-C, C-H (carbon) bond. In the VHB 4910, the explanation for its frequency-dependent dielectric response lies in the occurrence of a relaxation process due to the effect of orientation polarisation in the presence of the electric field [36].
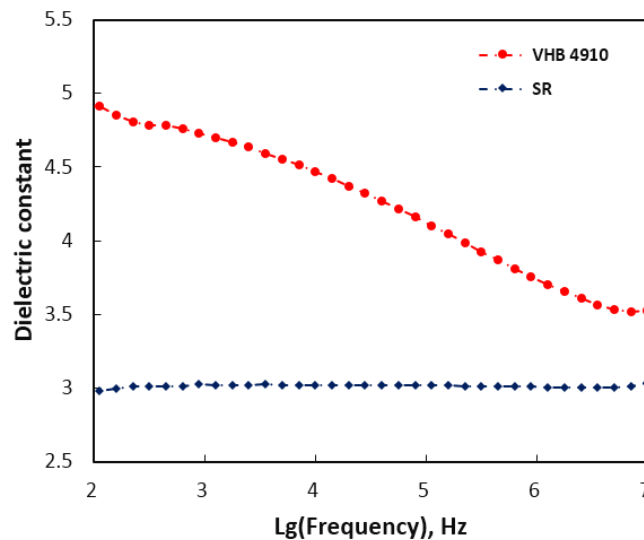

Fig. 3 Plots of dielectric constant versus frequency

Fig. 4 shows the relation between equi-biaxial stretch ratio and true stress. As can be seen from this figure, the true stress of pure SR (0.36 MPa) was higher than that of VHB 4910 (1.8 MPa) at a stretch ratio of 2.5. The increase of true stress with increasing

stretch ratio in SR was remarkably more pronounced than that of VHB 4910 indicating a more rapid stiffening effect in pure SR, which is favorable for suppressing EMI. The required true stress to achieve the same stretch ratio for pure SR was lower than that of VHB 4910 at stretch ratios below 1.6 while it was higher than that of VHB 4910 beyond stretch ratios of 1.6.
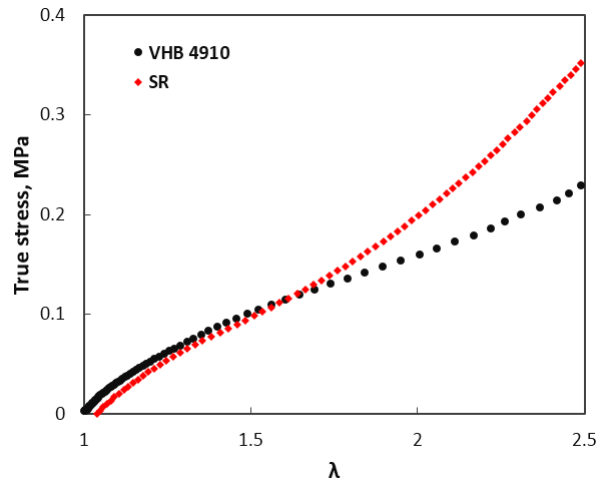

Fig. 4 The relation between true stress and stretch ratio

As reported in earlier research [37], EMI can be eliminated by controlling the strain-stiffening effect. It is well known that the stiffness of polymer materials can be characterised by tangent modulus, hence the strain-stiffening effect can be described by obtaining the relation between stretch ratio and tangent modulus. Fig. 5 shows the evolution of tangent modulus with increasing stretch ratio. As can be observed from this figure, for both pure SR and VHB 4910, tangent modulus decreased and then increased with the increase of stretch ratio. At a specific stretch ratio, tangent modulus reached a minimum indicating the lowest stiffness for each material. For VHB 4910, the lowest tangent modulus was about 0.10 MPa at a stretch ratio of about 2, while the lowest tangent modulus of pure SR was about 0.17 MPa at the lowest stretch ratio of about 1.5.
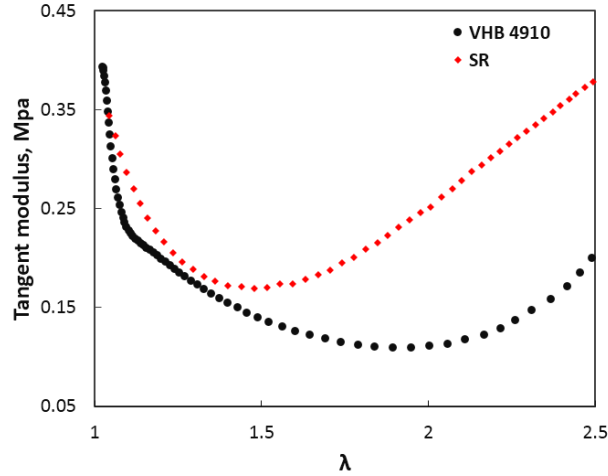
Fig. 5 Plots of tangent modulus dependency on stretch ratio

The relation between applied voltage and actuated stretch ratio is shown in Fig. 6. As can be seen from the figure, without pre-stretch, the VHB 4910 film achieved a very small equi-biaxial stretch ratio by applying a high voltage of about 10 kV in the experiment. However, it can be seen from the curves plotted with both equations from the Suo and Li models that the actuated stretch ratio increased with an increase in voltage up to the peak and then diminished. In a typical experiment, the voltage was programmed to ramp up slowly. When it reached a local maximum with a much larger stretch ratio, no state of equilibrium existed in the vicinity of this maximum as the voltage increased further. In this circumstance, EMI occurs [34]. The Suo model ignored the influence of stretch on the dielectric constant of a DE material. By using this model, when VHB 4910 was applied with a pre-stretch ratio of 1.6, the voltage increased as stretch ratio increased and reached a plateau beyond a stretch ratio of about 2. When a pre-stretch ratio of 2 was applied, voltage increased with an increase in stretch ratio until the stretch ratio reached 2.5. The Li model included a consideration of the influence of stretch on the dielectric constant of DE materials. By using the Li model, the voltage increased and then decreased with increasing stretch ratio when a pre-stretch ratio of 1.6 was applied. When a pre-stretch ratio of 2 was applied to the material, the voltage increased with increasing stretch ratio and a plateau was almost reached at a stretch ratio of 2.5. The experimental data for VHB4910 from this research was located between the two plotted curves derived from the Suo and Li models

respectively. The reason for this was probably because the pre-stretch frame used and/or the compliant electrode layer which restrained further deformation of the VHB 4910 film.
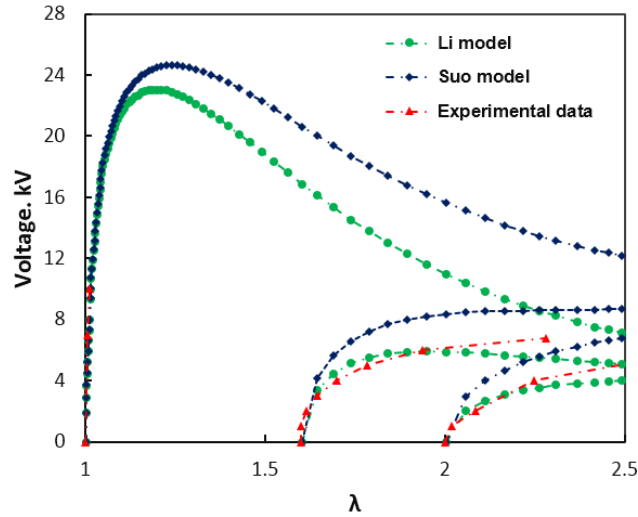

Fig. 6 Plots of voltage related to stretch ratio for VHB 4910

Fig. 7 shows the plots of voltage with stretch ratio for pure SR, both curves derived from the Suo model and experimental data are presented. As the dielectric constant of SR is independent of stretch due to the absence of Maxwell polarization [38], the simulation using the Li model, which considered the effect of stretch on dielectric constant, is not described here. Simulation curves from the Suo model in Fig. 7 show that without pre-stretch, the EMI for a 300 μm-thick SR membrane occurred at a voltage of about 9 kV for an equi-biaxial stretch ratio of 1.21. However, breakdown failure took place at a stretch ratio of 1.02 by applying a voltage of 2.5 kV in the experiment. At a pre-stretch ratio of 1.6, the simulated curve reached a plateau at a voltage of about 4.5 kV, while the SR sample failed at a voltage induced stretch ratio of 1.8 under a voltage of 3.8 kV. Finally, EMI for the SR thin film was eliminated by applying a pre-stretch ratio of 2.0. The SR specimen achieved a voltage induced stretch of 2.3 at a voltage of 3.2 kV.
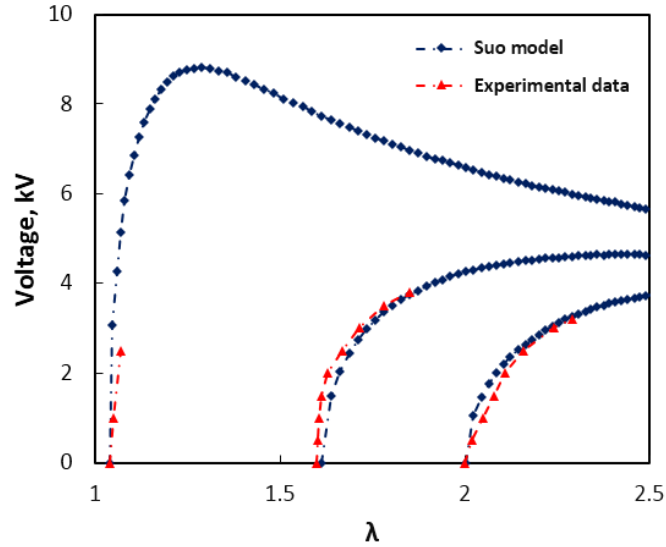
Fig. 7 Plots of voltage related to stretch ratio for pure SR

Conclusions

Both acrylate VHB 4910 and SR can achieve large voltage induced stretch ratios. Equi-biaxial tensile testing showed that pure SR exhibited a strain-stiffening effect at a smaller stretch ratio than for VHB 4910. SR based DEs required a lower electric field to achieve a large voltage-induced deformation and to exhibit the elimination of EMI. Hence, SR is a promising candidate for DE materials in terms of its general electromechanical performance and the elimination of EMI.

Acknowledgements

Conflicts of interests

The authors declare that they have no conflict of interest.

References

[1] R. Pelrine, R. Kornbluh, Q. Pei, J. Joseph, High-Speed Electrically Actuated Elastomers with Strain Greater Than 100%, Science, 287 (2000) 836-839.

[2] P. Brochu, Q. Pei, Advances in Dielectric Elastomers for Actuators and Artificial Muscles, Macromolecular Rapid Communications, 31 (2010) 10-36.

[3] J.-S. Plante, S. Dubowsky, On the performance mechanisms of Dielectric Elastomer

Actuators, Sensors and Actuators A: Physical, 137 (2007) 96-109.

[4] C. Keplinger, T. Li, R. Baumgartner, Z. Suo, S. Bauer, Harnessing snap-through instability in soft dielectrics to achieve giant voltage-triggered deformation, Soft Matter, 8 (2012) 285-288.

[5] M. Giousouf, G. Kovacs, Dielectric elastomer actuators used for pneumatic valve technology, Smart Materials and Structures, 22 (2013) 6.

[6] S. Son, N.C. Goulbourne, Dynamic response of tubular dielectric elastomer transducers, International Journal of Solids and Structures, 47 (2010) 2672-2679.

[7] K. Daheshpour, S. Jalali Mazlouman, A. Mahanfar, J.X. Yun, X. Han, C. Menon, F. Carpi, R.G. Vaughan, Pattern reconfigurable antenna based on moving V-shaped parasitic elements actuated by dielectric elastomer, Electronics Letters, 46 (2010) 886-888.

[8] K. Jung, K.J. Kim, H.R. Choi, A self-sensing dielectric elastomer actuator, Sensors and Actuators a-Physical, 143 (2008) 343-351.

[9] S. Shian, K. Bertoldi, D.R. Clarke, Dielectric Elastomer Based "Grippers" for Soft Robotics, Advanced Materials, 27 (2015) 6814.

[10] M. Babič, R. Vertechy, G. Berselli, J. Lenarčič, V. Parenti Castelli, G. Vassura, An electronic driver for improving the open and closed loop electro-mechanical response of Dielectric Elastomer actuators, Mechatronics, 20 (2010) 201-212.

[11] K. Ren, S. Liu, M. Lin, Y. Wang, Q.M. Zhang, A compact electroactive polymer actuator suitable for refreshable Braille display, Sensors and Actuators A: Physical, 143 (2008) 335-342.

[12] T. McKay, B. O'Brien, E. Calius, I. Anderson, Self-priming dielectric elastomer generators, Smart Materials and Structures, 19 (2010) 055025.

[13] S. Chiba, M. Waki, R. Kornbluh, R. Pelrine, Extending applications of dielectric elastomer artificial muscle, Proc. SPIE 6524, Electroactive Polymer Actuators and Devices (EAPAD) 2007, 652424.

[14] L.J. Romasanta, M.A. Lopez-Manchado, R. Verdejo, Increasing the performance of dielectric elastomer actuators: A review from the materials perspective, Progress in Polymer Science, 51 (2015) 188-211.

[15] X. Zhao, Z. Suo, Electromechanical instability in semicrystalline polymers, Applied Physics Letters, 95 (2009) 1945.

[16] X. Zhao, Z. Suo, Electrostriction in elastic dielectrics undergoing large deformation, J. Appl. Phys., 104 (2008) 123530.

[17] J.-S. Plante, S. Dubowsky, Large-scale failure modes of dielectric elastomer actuators, International Journal of Solids and Structures, 43 (2006) 7727-7751.

[18] D.D. Tommasi, G. Puglisi, G. Saccomandi, G. Zurlo, Pull-in and wrinkling instabilities of electroactive dielectric actuators, Journal of Physics D: Applied Physics, 43 (2010) 325501.

[19] R. Shankar, T.K. Ghosh, R.J. Spontak, Dielectric elastomers as next-generation polymeric actuators, Soft Matter, 3 (2007) 1116-1129.

[20] J. Sheng, H. Chen, L. Liu, J. Zhang, Y. Wang, S. Jia, Dynamic electromechanical performance of viscoelastic dielectric elastomers, Journal of Applied Physics, 114 (2013) 034119.

[21] S. Rosset, B.M. O'Brien, T. Gisby, D. Xu, H.R. Shea, I.A. Anderson, Self-sensing dielectric elastomer actuators in closed-loop operation, Smart Materials and Structures, 22 (2013) 104018.

[22] R. Pelrine, R. Kornbluh, G. Kofod, High-Strain Actuator Materials Based on Dielectric Elastomers, Advanced Materials, 12 (2000) 1223-1225.

[23] Z. Zhang, L. Liu, J. Fan, K. Yu, Y. Liu, L. Shi, J. Leng, New silicone dielectric elastomers with a high dielectric constant, Proc. SPIE 6926, Modeling, Signal Processing, and Control for Smart Structures 2008, 692610.

[24] L. Yanju, L. Liwu, Z. Zhen, L. Jinsong, Dielectric elastomer film actuators: characterization, experiment and analysis, Smart Materials and Structures, 18 (2009) 095024.

[25] X. Zhao, Q. Wang, Harnessing large deformation and instabilities of soft dielectrics: Theory, experiment, and application, Applied Physics Reviews, 1 (2014) 021304.

[26] Z. Suo, Theory of dielectric elastomers, Acta Mechanica Solida Sinica, 23 (2010) 549-578.

[27] B. Li, H. Chen, J. Qiang, S. Hu, Z. Zhu, Y. Wang, Effect of mechanical pre-stretch

on the stabilization of dielectric elastomer actuation, Journal of Physics D: Applied Physics, 44 (2011) 155301.

[28] X.-M. Wang, H. Li, Z.-N. Yin, H. Xiao, Multixial strain energy funcgtions of rubberlike materials: an explicit approach based on polynomial interpolation, Rubber Chemistry and Technology, 87 (2014) 168-183.

[29] M. Wissler, E. Mazza, Modeling of a pre-strained circular actuator made of dielectric elastomers, Sensors and Actuators A: Physical, 120 (2005) 184-192.

[30] P.A.L.S. Martins, R.M. Natal Jorge, A.J.M. Ferreira, A Comparative Study of Several Material Models for Prediction of Hyperelastic Properties: Application to Silicone-Rubber and Soft Tissues, Strain, 42 (2006) 135-147.

[31] M. Rachik, F. Schmidtt, N. Reuge, Y. Le Maoult, F. Abbeé, Elastomer biaxial characterization using bubble inflation technique. II: Numerical investigation of some constitutive models, Polymer Engineering & Science, 41 (2001) 532-541.

[32] O. Yeoh, P. Fleming, A new attempt to reconcile the statistical and phenomenological theories of rubber elasticity, Journal of Polymer Science-B-Polymer Physics Edition, 35 (1997) 1919-1932.

[33] X.H. Zhao, Z.G. Suo, Theory of Dielectric Elastomers Capable of Giant Deformation of Actuation, Physical Review Letters, 104 (2010) 4.

[34] T. Lu, J. Huang, C. Jordi, G. Kovacs, R. Huang, D.R. Clarke, Z. Suo, Dielectric elastomer actuators under equal-biaxial forces, uniaxial forces, and uniaxial constraint of stiff fibers, Soft Matter, 8 (2012) 6167-6173.

[35] C. Jean-Mistral, T. Vu-Cong, A. Sylvestre, On the power management and electret hybridization of dielectric elastomer generators, Smart Materials and Structures, 22 (2013) 12.

[36] R. Xiao, X. Gou, W. Chen, Suppression of electromechanical instability in fiber-reinforced dielectric elastomers, AIP Advances, 6 (2016) 035321.

[37] F.B. Madsen, L. Yu, A.E. Daugaard, S. Hvilsted, A.L. Skov, A new soft dielectric silicone elastomer matrix with high mechanical integrity and low losses, RSC Advances, 5 (2015) 10254-10259.